



**Acoustics'08
Paris**
June 29-July 4, 2008

www.acoustics08-paris.org

euonoise

A time domain model of scattering from small discrete volume particles: tank validation

Gaetano Canepa^a, Jean-Pierre Sessarego^b, Alessandra Tesei^a, Régine Guillermin^b and Raymond Soukup^c

^aNATO Undersea Research Centre, Viale San Bartolomeo 400, 19126 La Spezia, Italy

^bLaboratory for Mechanics and Acoustics CNRS, 31 chemin Joseph Aiguier, 13009 Marseille, France

^cU.S. Naval Res. Lab., Acoust. Div., Code 7142, 4555 Overlook Ave. SW, Washington, DC 20375, USA

canepa@nurc.nato.int

A time domain model of scattering from small discrete particles embedded in a sediment volume is presented here with an experimental validation. The model is implemented on the backbone of the BORIS-3D model which originally included only surface scattering and volume scattering from small perturbations of the volume density and sound speed. The proposed model adds discrete volume scatterers and simulates both monostatic and bistatic configurations. The experimental data for validation were collected in a tank using a silicon plate (with a flat upper interface) in which 10% of the volume is occupied by spherical glass beads 1 mm in diameter. This work is focused on the time domain evolution of the scattered echo. The results shows a very good agreement between simulated and experimental data in both amplitude and shape.

1 Introduction

In the field of high frequency acoustics volume scattering by discrete particles is generally modeled [1] by using the integral of volume scattering cross section, which is a major simplification of the acoustic response and does not provide information on time dependence, coherence and other geometrical effects. This paper considers a new approach based on BORIS-3D [2, 3, 4], a time domain modeling tool which, given the geometry setup, the TX/RX sonar characteristics, the pulse waveform and the geophysical properties of water and sediment, predicts the scattered signal. The original model includes surface scattering, based on Kirchhoff approximation (KA), and volume scattering, based on small perturbations (SP) approximation. BORIS-3D has then been improved with the capability to simulate surface scattering of higher order (small slope approximation of order 2 and 4) [5, 6]: the new version of the tool is called BORIS-SSA. A model of scattering from volume discrete scatterers (particles) has been recently added to the original SP volume scattering and is briefly described here. To validate this new modeling tool, a tank experiment was conducted at the CNRS/LMA in December 2007. The major advantage of model validation through tank experiment data is the possibility to control the experiment geometry and the repeatability, and to limit the complexity of the sediment. On the basis of the data collected in a well controlled tank experiment, it is shown here that the modified version of BORIS-SSA is able to model both in amplitude and in shape, even small features of the backscattering and bistatic scattering response by a flat silicon model of a muddy sediment with inclusions. This is the minimal pre-requisite for a model to be able to predict at-sea data. This paper focusses only on the model validation of the monostatic configuration.

2 Model description

The SP volume scattering included in BORIS-SSA is computed by decomposing the sound field into rays, each of which connects the source to one element of surface. The ray is then scattered by the surface but also partially transmitted into the sediment. The sediment properties are given in terms of average sound speeds and density values and of a three-dimensional matrix which contains the small perturbation of sediment sound speed and density. The SP scattered field is calculated by summing all the interactions of each ray with the volume matrix elementary components [2] (Fig. 1). The difference in pulse frequency contents caused by

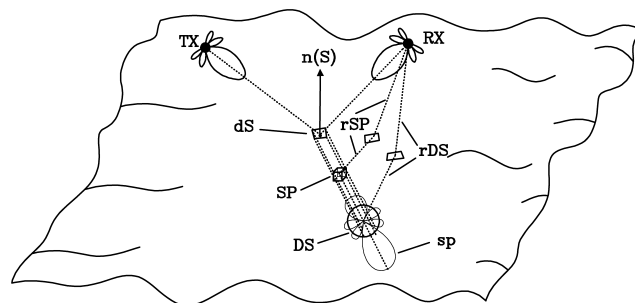


Figure 1: A schematic of the contribution to the bistatic signal scattered from a seabed. In the figure: **TX** is the transmitter, **RX** the receiver, **dS** an elemental surface element, **SP** an elemental volume contributing to small perturbation volume scattering, **DS** a particle contributing to the discrete volume scattering, **sp** the **DS** particle scattering pattern, **rSP** and **rDS** are scattered paths from **SP** and **DS** to **TX** considering the surface flat.

attenuation in the sediment are also taken into account and the contributions are added up taking into account the different travel time. Both monostatic and bistatic configurations can be defined.

The contribution to volume scattering by small particles is included in the following way. Only spherical particles are simulated, with multiple scattering between particles only included in the value of the attenuation by using Eqn. (3.25) in [7]. These approximations do not restrict the applicability of the model too much. On the other hand, the model is implemented in such a way that particles with different radius can be used. They can be rigid, elastic or empty; particles with a thin shell can also be added. The 3D-scattering pattern of each of the particles is calculated based on an analytical approach [8].

The model is implemented by using a second three-dimensional matrix, in which each element occupied by a spherical particle contains the pointer to the scattering pattern of the given particle and to its properties (center position and cross section). Along the propagation into the sediment, the ray scattering is calculated with the SP scattering model. Each time a ray hits a sphere, a scattering component is calculated as generated by the center of the sphere with an intensity proportional to the ray cross section divided by the sphere cross section. The scattering contribution is also weighted by the scattering pattern in the direction of the path from the sphere center to the receiver.

The simulation time of the new algorithm has in-

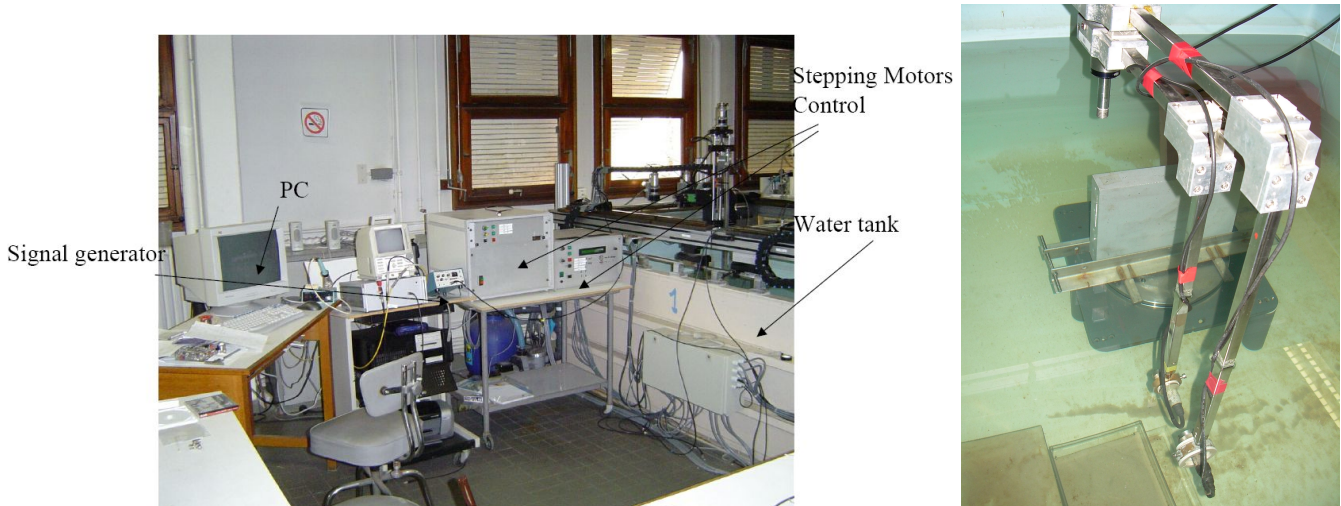


Figure 2: Photos of the experimental setup. Left: the acquisition system; right: the silicone slab inside the tank with the TX and RX transducers (setup for bistatic measurements).

created by only $\approx 1\%$ with respect to the SP code, as the difference in elemental volume contributions are minimal (the time consuming part, the scattering pattern and the particle distribution, being pre-computed).

3 Experimental setup

The experimental setup has already been described in [9, 10, 11], where results and details on configuration and parameters are provided. Figure 2 shows the automated system and the tank configuration used to acquire the data (water sound speed 1479.546 m/s). The TX/RX transducers are two Panametrics-NDT V301 (nominal diameter 2.54 cm, 500 kHz [12]). The sediment model is a slab of silicon (density $\rho=1251 \text{ kg/m}^3$, compressional sound speed $c_p=1020 \text{ m/s}$, shear sound speed $c_s \approx 0 \text{ m/s}$, compressional attenuation $\alpha=41 \text{ Np/m}$, dimension $30 \times 30 \times 5.2 \text{ cm}$) filled with 10% by volume of glass beads (diameter 1 mm, $\rho=2539 \text{ kg/m}^3$, $c_p=5231 \text{ m/s}$, $c_s=3124 \text{ m/s}$). The surface of the slab is flat. Figure 3 shows an X-ray scan of the slab and a plot of the bead density *versus* depth in the slab. The density plot is obtained by elaborating data from 74 X-ray scans and clearly shows that the bead density is lower near the upper surface than in the bulk of the slab.

Two sets of measurements are performed:

- the measurement of the backscatter signal for incident angles varying from 0° to 70° with 10° step.
- The measurement of the bistatic scattering signal with source at normal incidence and receiver observation angles varying from 10° to 70° , with 10° step.

Thirty different sonar positions are chosen along the slab to obtain mean and variance of the scattering curves. The mechanical system is set in such a way that rotations of the transducers always happen with respect to the same point on the surface of the slab.

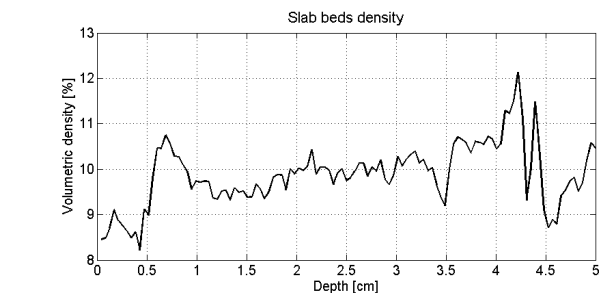
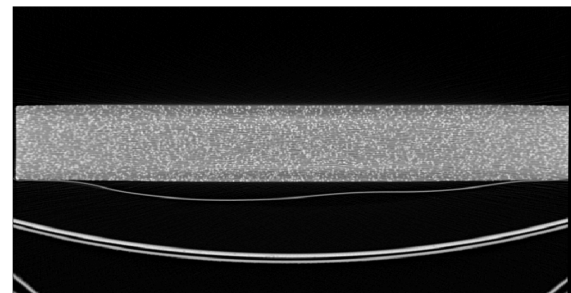


Figure 3: Top: X-rays scan of the slab with beads. Bottom: concentration (volume percentage) of the glass beads as estimated from the X-rays scan images.

4 Simulation setup

The geometry of the angular configuration between sonar and sample is taken as exact. The transducer to sample distance is estimated by measuring the time of flight (maximum error $\approx 1.5 \text{ mm}$).

4.1 Transmit/receive beam patterns

The TX and RX beam patterns of the cylindrical transducer can be set using the equation for a circular plane array [13]: $D(\theta) = 2J_1(\pi D \sin \theta / \lambda) / (\pi D \sin \theta / \lambda)$, where D is the transducer diameter, θ is the angle at which the beam pattern is evaluated, and λ is the sound wavelength in water.

4.2 Pulse shape

The actual transmitted pulse shape at 500 kHz is not easy to determine. Moreover, the effect of the RX transducer on the received signal is important to evaluate. The transmitted pulse has been measured under the same geometrical conditions as the experiments, using the RX transducer to receive the pulse. The calibrated pulse will be different from the transmitted one but, if a linear model and linear RX transducer are used, there should be no differences between experimental and simulated data. The calibration suitable for backscattering configuration has been conducted pointing the TX/RX transducer directly to the water/air interface at the same distance used during the experiment with the slab of silicon. The transmitted pulse (including the effect of the RX transducer transfer function) is obtained by multiplying the shape of the received signal by two times the distance between the TX/RX transducer and the water air interface. All the data (simulated and experimental) are re-scaled based on the calibration signals.

A simulation of the normal backscattering from the water/air interface exhibits a perfect inverted replica of the transmitted pulse.

4.3 Slab parameters

After geometry and transducer parameters are defined the sediment/slab interface is acoustically characterized.

4.3.1 Sound speed and density

Serrarego *et al.* showed in [10] that the curve of the average reflection coefficient versus angle is not affected (between 5 and 75°) by the presence of 10% glass beads in the matrix of silicon, except for a higher variability with respect to the average value. As a consequence the sound speed and the density of the sediment (the most important parameters affecting the reflection coefficient) are maintained un-modified with respect to the pure silicon one (ρ , c_p and $c_s \approx 0$ reported in Sec. 3). A simulation of the experiment reported in reference [10], used to measure the reflection coefficient, has been carried out: the result exactly fits the reflection coefficient in the reference.

4.3.2 Compressional wave attenuation

An important parameter for sediment volume scattering is the attenuation of the compressional wave in the medium. Following Waterman and Truell [7], the inclusion of glass beads should increase the natural attenuation of the medium from 18 to 55*** Np/m. Direct measurements of the attenuation give a much higher attenuation, namely between 150 and 200Np/m. This higher value can be explained by two concurrent problems in the slab:

- the presence of a layer zone of higher concentration of beads, in which the attenuation is stronger, and
- the presence of small (diameter < 0.1 mm) air bubbles in the silicon matrix.

Big air bubbles (diameter > 1 mm) are visible in the X-ray images of the sample slab with no beads [11] and the presence of small bubbles is, as a consequence, highly probable. It has also to be considered that the addition of glass beads is likely to involve the inclusion of a higher concentration of small air bubbles in the silicon slab. On the other hand, the attenuation in the slab being so high, only a surficial layer will influence the scattered signal. But, near the surface both glass beads (see Fig. 3, bottom) and air bubbles (by natural migration) have a lower concentration. To determine the most suitable value of the attenuation to use, the time decay of the volume scattering component has been observed in the case of normal incidence backscattering. The value that matches the experimental data is 80 Np/m (compare the simulated and the experimental signal at 0° in Fig. 5).

4.3.3 Bead concentration

The concentration of the discrete glass beads in the sediment is setup following the plot in Fig. 3 (bottom). In the same time a 0.01***% of air bubble 30 μ m in diameter is added to the volume in such a way to obtain a theoretical value of the attenuation of 80*** Np/m (following [7]). If no air bubbles were included, the value of the simulated scattering resulted much lower than the measured one.

5 Results

5.1 Amplitude angular dependency

The comparison between experiment and simulation of the scattering amplitude angular dependency is shown in Fig. 4. The scattering amplitude is calculated with the following equation for both simulated and experimental data: $20 \log_{10}(\frac{E_s(\alpha)}{E_0})$. E_0 and E_s are the average of the absolute value of the Fourier transform of the calibration and the scattered signal in the band 450–550 kHz. The average on a 10% band is chosen to reduce the scattering amplitude variation associated to a single frequency spectral contribution. The discrepancy between the simulated and experimental average amplitude is within 3 dB, and remains within 4 dB at higher incident angles. This differences are well inside the error bar associated with this type of data.

5.2 Time domain shapes

The normalized shapes of the experimental scattered signal at different angles are compared with simulated data (Fig. 5). Signals are normalized to remove the amplitude differences due to the large variance of the scattered echo. It appears that the shape of the simulated signal does not differ from to the experimental one (in term of surface reflected component versus volume scattering and in terms of envelope of the signal).

6 Conclusion

Tank experiments generally allow for a well controlled environment. Notwithstanding this, even if most of the

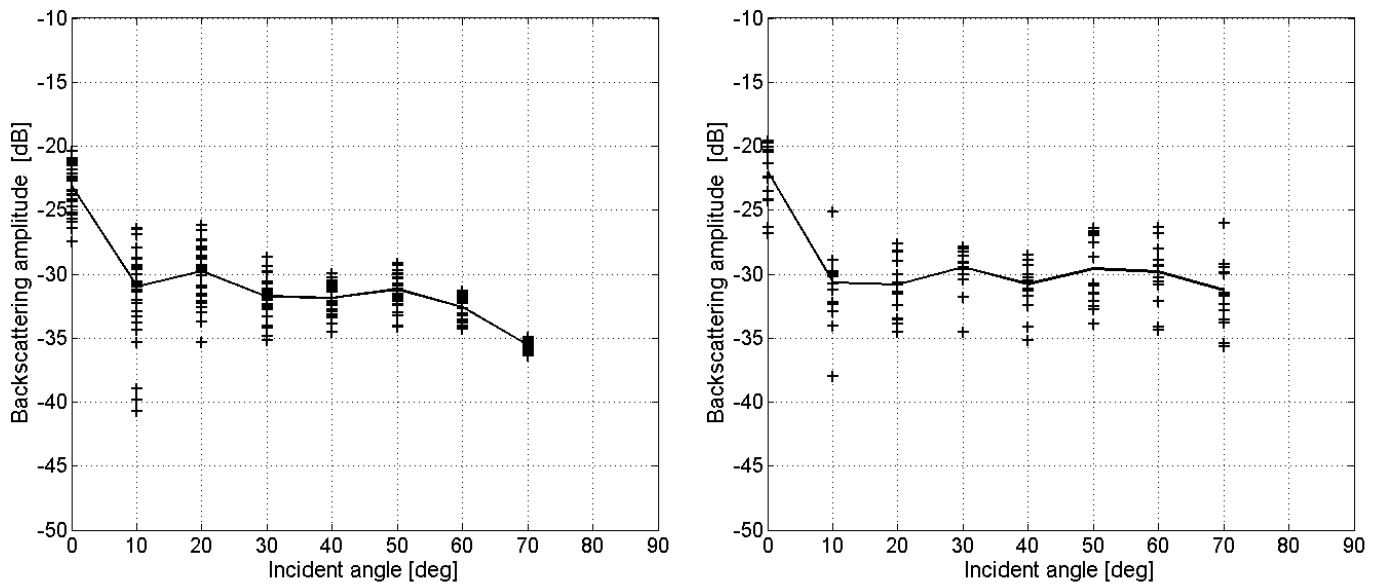


Figure 4: Experimental (left) and simulated (right) values of the scattering amplitude for different incident angle. The crosses give the amplitude for each position on the slab while the continuous line is the average.

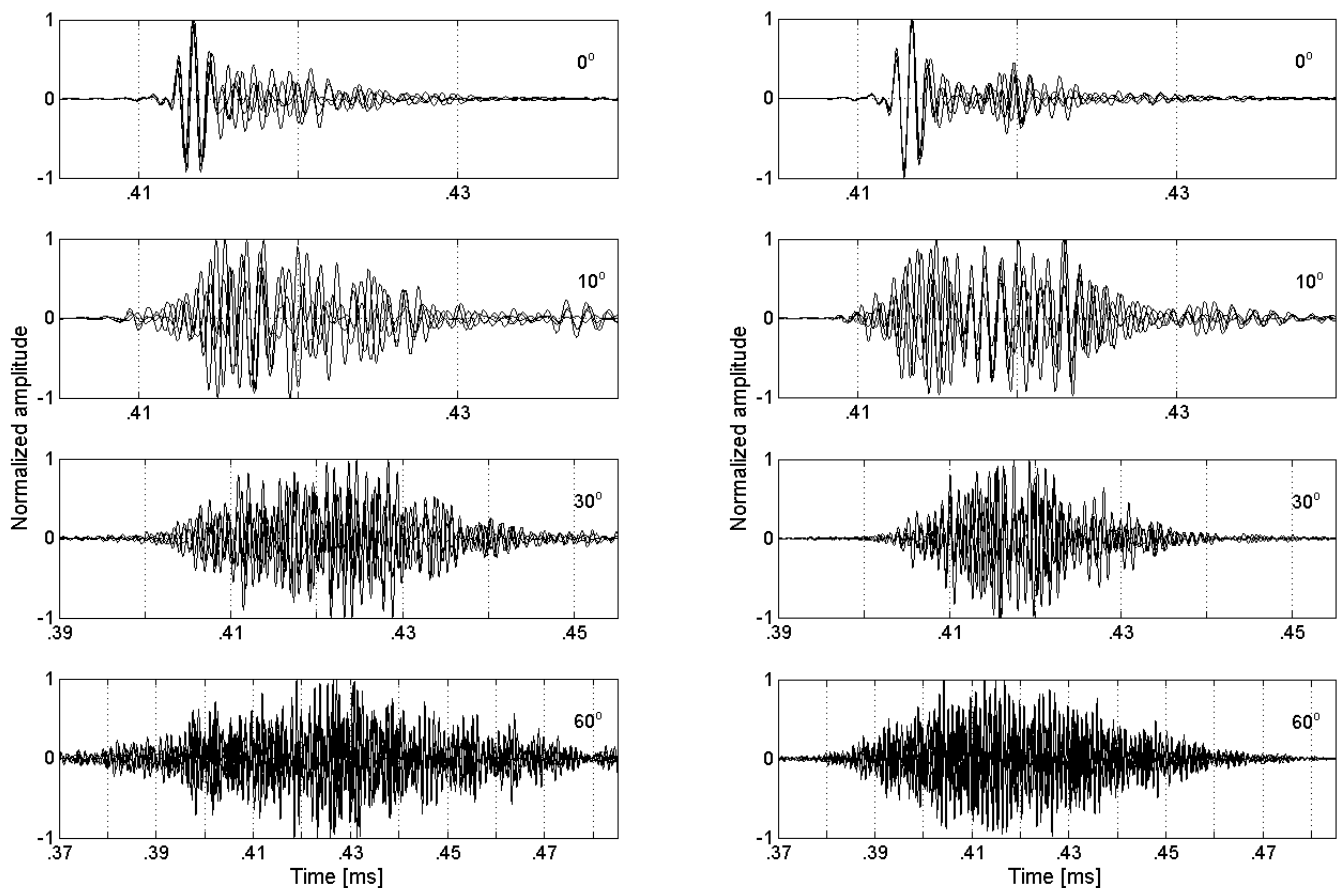


Figure 5: Experimental (left) and simulated (right) normalized time series at different angles. Four time series are overlapped for each angle. Only in the signal at 0° are the surface scattered components visible (in the first $5\mu s$ of the scattered signal).

model parameters are well known, some can be hard to control and measure, especially when they are related to manufacturing processes. A case in point was the attenuation and the distribution of glass and air scatterers in the sediment. Using experimental data it has been possible to evaluate the attenuation but the distribution of the scatterers in the sediment could only be guessed.

After these premises, the comparison of simulated with experimental data shows a remarkable agreement. The time series comparison is very good at all angles. The difference between the average curves of angular dependency of scattering amplitude is within 3 dB except beyond 60°.

This difference can be explained by the imperfect volume uniformity along the depth of the sediment model. A variability in the surficial bead distribution affect both attenuation and scattering at low grazing angle. Anyway, a model with a variable attenuation with depth cannot be tested with BORIS-SSA. In fact, the scattering modeling tool accepts only one value for the attenuation in the sediment. A further new version of BORIS-SSA will include the possibility to have any attenuation profile along the depth of the sediment with no increase in computation time and memory. The inclusion of a single Kirchhoff reflection layer inside the sediment (with no multiple reflection) will also be added. A wax sediment model, with uniform scatterer distribution and with no air bubbles included, is also under development in such a way to remove all the unknowns and problems tied to the silicon sediment model described here.

7 Acknowledgments

This work is supported, in the framework of a JRP, by the Office of Naval Research, the NATO Undersea Research Centre and the CNRS Laboratory of mechanical acoustics. The authors wish to acknowledge the contributions of Allen Reed of the Naval Research Laboratory for performing an X-ray analysis of a single sample and Finn Jensen and Mario Zampolli with their assistance in developing the JRP collaboration and for the fruitfully discussions.

References

- [1] D. R. Jackson and M. D. Richardson. *High-Frequency Seafloor Acoustics*. Underwater Acoustic. Springer, New York, 2007.
- [2] E. Pouliquen, O. Bergem, and N. G. Pace. Time-evolution modelling of seafloor scatter, part 1: Theory. Technical Report SM-0328, SACLANTCEN, La Spezia, Italy, 1997.
- [3] O. Bergem, E. Pouliquen, G. Canepa, and N. G. Pace. Time-evolution modelling of seafloor scatter, part 2; experimental verification. Technical Report SM-0327, SACLANTCEN, La Spezia, Italy, 1997.
- [4] G. Canepa, O. Bergem, and E. Pouliquen. The implementation of boris-3d: BOTTOM Response from Inhomogeneities and Surface version 1.0. Technical Report M-0125, SACLANTCEN, La Spezia, Italy, 1997.
- [5] G. Canepa, L. Pautet, and E. Pouliquen. Manual of boris-ssa: Bottom response from inhomogeneities and surface using small slope approximation. Memorandum M-0152, NATO URC, 2005.
- [6] R. J. Soukup, G. Canepa, H. J. Simpson, J. E. Summers, and R. F. Gragg. Small-slope simulation of acoustic backscatter from a physical model of an elastic ocean bottom. *JASA*, 122:2551–2559, 2007.
- [7] P. C. Waterman and R. Truell. Multiple scattering of waves. *J. Math. Phys.*, 2(4):512–537, 1960.
- [8] R. R. Goodman and R. Stern. Reflection and transmission of sound by elastic spherical shells. *JASA*, 34:338–344, 1962.
- [9] J-P. Sessarego, J. Sageoli, and C. Pinhède. Analyse de milieux inhomogènes en réflexion et en rétrodiffusion à partir de mesures en laboratoire. Technical Report Rapport intermédiaire, IFREMER, Brest, France, 1999.
- [10] J-P. Sessarego and P. Sanchez. Use of scaled models to study high frequency sea floor backscattering. In N. G. Pace and P. Blondel, editors, *Boundary influences in high frequency, shallow water acoustic*, pages 209–216, Bath, UK, 2005.
- [11] J-P. Sessarego, J. Sageoli, and C. Pinhède. Analyse de milieux inhomogènes en réflexion et en rétrodiffusion à partir de mesures en laboratoire. Technical Report Rapport final Contract IFREMER-CNRS 98.2.311333, IFREMER, Brest, France, 2000.
- [12] Olympus NDT. *Ultrasonic Transducers for Non-destructive Testing*, 2006. Available electronically at: <http://www.olympusndt.com/data/File/panametrics/panametrics-UT.en.pdf>.
- [13] X. Lurton. *An introduction to underwater acoustics*. Springer-Praxis books in geophysical Sciences. Springer-Praxis, 2002.